TELEANALYSIS, GEOLOGICAL AND STRUCTURAL MAPPING OF THE SOUTHERN ZONE OF THE TIBESTI METALLOGENIC PROVINCE (NORTHERN CHAD)

[1]DOUMNANG MBAIGANE Jean Claude, [1]MBAGUEDJE DIONDOH, [1]Léontine TEKOUM, [1]Ngaro MBAITI, [2]Pierre ROCHETTE

[1]Laboratoire de Géologie, Géomorphologie et Télédétection, Département de Géologie, F.S.E.A., Université de N'Djamena, B.P. 1027, rue de Farcha, N'Djamena, Tchad.
[2]Centre de recherche et d'enseignement des géosciences de l'environnement (CEREGE) Aix Marseille Université. Av Louis Philibert, 13100 Aix-en-Provence, France.

DOI: https://doi.org/10.56293/IJASR.2024.6217

IJASR 2024
VOLUME 7
ISSUE 6 NOVEMBER – DECEMBER **ISSN: 2581-7876**

Abstract: The Tibesti massif is a Tertiary-Quaternary volcanic region underlain by Precambrian bedrock. The massif lies to the south of the Sahara Desert. It has a very rugged topography, with the highest peak being Emi Koussi at 3,415 m. The geological map of the region dates back to the 1960s, and very little geological work has been carried out. Since the 1970s, repeated wars in the region have made access difficult for scientific work because of the anti-personnel mines hidden throughout the area. Using aerial photography, Landsat images and remote sensing techniques, in particular Landsat 7 ETM+ satellite image processing and analysis, with ENVI 4.5 and QGIS software, we have updated a geological and structural map of this difficult-to-access region.

Based on the coloured compositions and channel ratios, a lithology was determined:

- two types of Palaeozoic sandstone characterised by two different drainage network textures;
- Tertiary and Quaternary rhyolites and basalts.
- The lineaments were highlighted using the Lapalacian filter, QGIS 3.28 and 3DEM:
- Tectonic structures have been determined.
- A major NW-SE fault runs along the southern edge of the massif. This fault can be seen in the colour composition of the various raw and processed channels; it has been confirmed by a digital terrain model (DTM),
- a NW-SE-trending sinister drop separates the Upper Tibestian and Lower Tibestian formations.

A detailed 1:100,000 geological map of the southern Tibesti massif was produced from analyses and interpretations of processed Landsat images and aerial photographs.

The processing of these data has highlighted the lineaments and different types of faults that have affected the geological formations of the Tibesti. A structural diagram of the southern Tibesti massif has been produced.

This mapping work will help to guide hydrogeological research in this austere area and mining research in this province, which is rich in minerals but little explored.

Keywords: remote sensing, mapping, metallogenic province, Tibesti, Chad.

INTRODUCTION

The Tibesti volcanic massif is located in a desert zone in the far north of Chad. It was first studied by Wacrenier (1958), who drew up one of the first geological maps of the region. Vincent (1963, 1995) studied the various volcanoes in the massif from a magmatic point of view.

Because of its geographical location, its very hostile desert climate, the lack of road infrastructure and the many wars that have taken place since the 1970s, the Tibesti massif has been little studied.

The Tibesti volcanic massif was chosen as a study area to contribute to our knowledge of the region's geology using satellite data. The aim of this study is to use remote sensing applied to geology (Hunt et al., 1973; 1974; Scanvic, 1983; Gupta, 1991; Scanvic, 1992): to map and structure the Tibesti massif; to relate it to continental fault zones. This isolated area in the middle of the desert has not been studied since the 1960s. The Tibesti region has been the subject of numerous wars in Chad and has been difficult to access since the 1970s, due to the very rugged terrain and the anti-personnel mines that have not been destroyed until now. The best-known maps of the Tibesti massif are those of the Central Sahara expeditionaries: Thilo (1920), Grove (1960), Furon (1963), Grove and Warren (1968). The most recent geological maps of Chad proper were acquired in the 50s and 60s (Wacrenier et al., 1958; Wolff, 1964).

The Tibesti volcanic massif is made up of several volcanic craters, the highest of which (Emi Koussi) reaches an altitude of 3,415 m (Dalloni, 1936; Vincent, 1963; Pegram et al., 1976; Mohamed and Seyd, 1982; Mohammad, 1986; Dieter, 1982). Volcanic activity probably began as early as the Eocene with the outpouring of basalts, followed by a very complex succession of acid lavas (rhyolites) (Wacrenier et al., 1957; Vincent., 1963; Bruschek, 1974; 1982) and continues to this day with post-volcanic phenomena: fumaroles, solfataras and thermal springs (Hisseine, 1986).

Chad and neighbouring countries have engaged in artisanal and semi-industrial gold mining (Photo 1). This uncontrolled gold mining contributes enormously to environmental degradation. Tibesti has recognised metallogenic potential, but vast areas remain unexplored. Little is known about the geology of Tibesti. A detailed geological map of the province is still lacking, and modern exploration techniques (geophysics, geochemistry, remote sensing) have not been systematically applied to mineral exploration. Little information is available on the mineral reserves of the Tibesti province.

The aim of this study is to use remote sensing applied to geology. To produce a geological and structural map of the metallogenic province of the Tibesti massif. The maps produced will be used to guide research, exploration and the controlled exploitation of mineral and water resources.

I - GEOGRAPHICAL SITUATION

Chad is located in the heart of Africa, between the equator and the Tropic of Cancer, in the northern hemisphere, between 7° and 24° parallel of north latitude; 13° and 24° meridian of east longitude.

The study area, currently Tibesti province, is located in the former prefecture of Borkou Ennedi Tibesti (B.E.T.), between 17°10 and 18° East longitude and 20°30 and 21°10 North latitude. This area covers the south of the Tibesti massif on the one hand and the north-east of Borkou on the other. It covers an area of around 34,000 km2 (fig. 1).

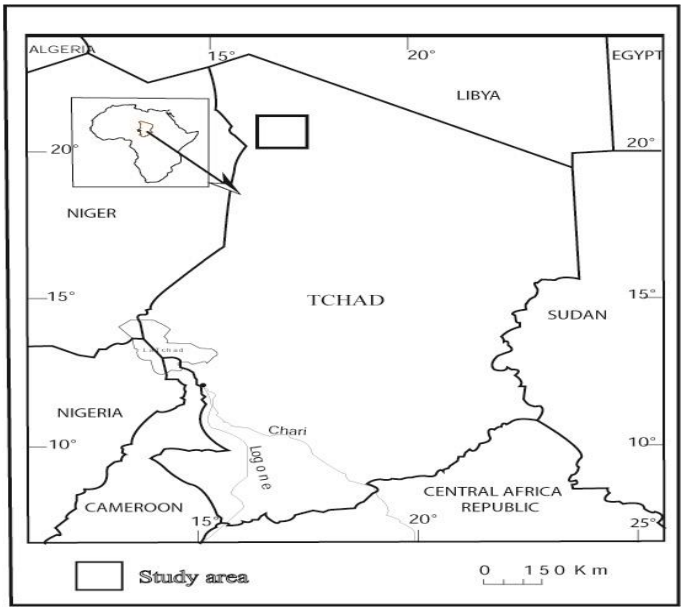

Figure 1. Map showing the geographical location of the study area.

II. GEOLOGICAL FRAMEWORK

The geology of Chad

Chad lies in the Central African belt, between the Congo craton, the Sahara metacraton and the West African craton (fig. 2).

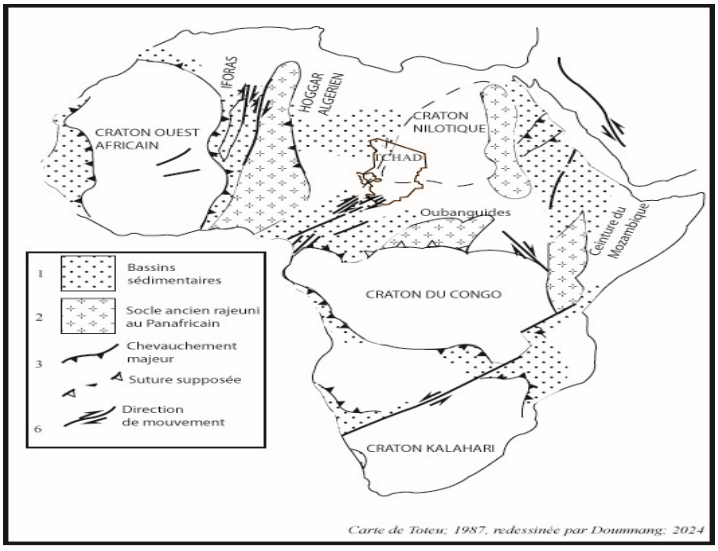

Figure 2. Map of Chad's position in the African cratons.

Chad's geological formations are composed of Precambrian rocks overlain by Phanerozoic volcanic and sedimentary rocks. The Precambrian crystalline basement is divided into several isolated massifs or geological units around the Chad Basin: the Tibesti massif in the far north of the country, the Ouddaï massif on Chad's eastern and central border, the Guéra massif in the centre, and the Yadé and Mayo Kebbi massifs in the south and south-west respectively (fig.3).

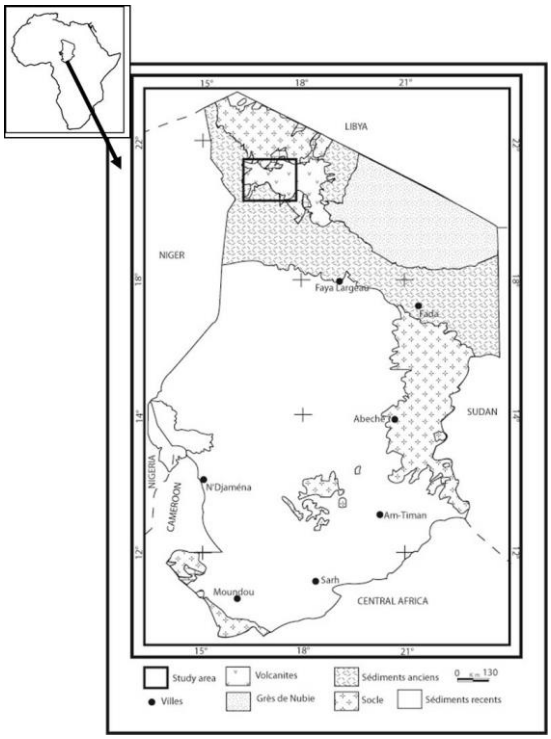

Figure 3: Synthetic geological map of Chad;

The Tibesti, Ouaddaï and Guéra massifs form the Eastern Sahara craton (Bertrand and Caby, 1978), the Sahara metacraton (Black and Liégeois, 1993) or the Saharan metacraton (Abdelsalam et al, 2002; 2011), made up of an amalgam of contemporary Archean rocks, structurally related to the Proterozoic or Archean, and which were strongly remobilised during the Pan-African orogeny of the Late Proterozoic (Pegram et al., 1976; Black et Liégeois, 1993, Abdelsalam et al., 2002; 2011), which constitute the basement (fig. 3 and fig. 4 A) . The Mayo Kebbi massif, in the south-western corner of Chad, consists of juvenile Neoproterozoic crust formed during and after the Pan-African orogeny (Kasser, 1998; Doumnang, 2006; Isseini, 2011; Mbaguedjé, 2015; Shellnutt et al., 2015) (Fig. 3). The Mbaibokoum massif or Yadé massif outcrops in the extreme south of Chad, near the Central African Republic border. This area was explored in the 1960s by geologists from the AEF. The Precambrian extends over an area of 8,000 km2, but outcrops very widely beyond the border to the south (Central African Republic, Cameroon). This massif has geological affinities with the Guéra massif and the southern part of the Ouaddaï massif. The main cartographic unit is a large batholith, consistent with the host rocks, which are made up of micaschists, quartzites and gneisses, crossed by granites. The age of the granites in the Yadé massif ranges from 600 to 580 Ma, similar to the Ouaddaï granites, and is also attributed to the Pan-African orogeny (Kusnir, 1993; Djekoundam, 1995).

The Chad region was tectonically stable after the Pan-African Orogeny, and sedimentary formations accumulated over most of its territory during the Palaeozoic (Bessole and Trompette, 1980; Schneider, 1992; Maurin, and Guiraud, 1993). These sediments are located in the northern and eastern parts of the territory, with younger sedimentation beginning in the Cretaceous and developing basins linked to horst and graben systems (Fig. 2), associated with the thinning of the Earth's crust and the extension linked to the break-up of the Gondwana supercontinent with the opening of the South Atlantic and the detachment of South America from the African continent (Guiraud et al, 1987 ; 1992 ; Maurin, and Guiraud, 1993 ; Isseini, 2011 ; Djerossem, 2020). Chad is a country with great unexplored and unexploited mining potential. This is due to a lack of targeted and focused research.

The Tibesti massif lies in the northern part of Chad, close to the Libyan border, and is geologically different from the other massifs surrounding the Chad Basin (Dalloni 1934; Wacrenier et al., 1958; Kaiser, 1972; Pegram et al., 1976;) (fig. 4 A). It consists of an ancient craton element with Proterozoic or Archean metamorphic rocks (Bruschek, 1974; 1982), heavily eroded from the transgressive Lower Palaeozoic, and a Miocene volcanic complex of several large stratovolcanoes (fig. 4 B) (Emi Koussi, Tarso Tiri, Tarso Tieroko, Tarson Voon, Tarso Yega, Tarso Abeki and Toussidé) (Dalloni.., 1936; Vincent, 1963; Mohamed and Seyd, 1982; Mohammad, 1982) with fragments of terrain dating back to the secondary period. The cratonic rocks are made up of two metamorphic series, separated by a level of conglomerate (Pegram et al., 1976) (Fig. 5).

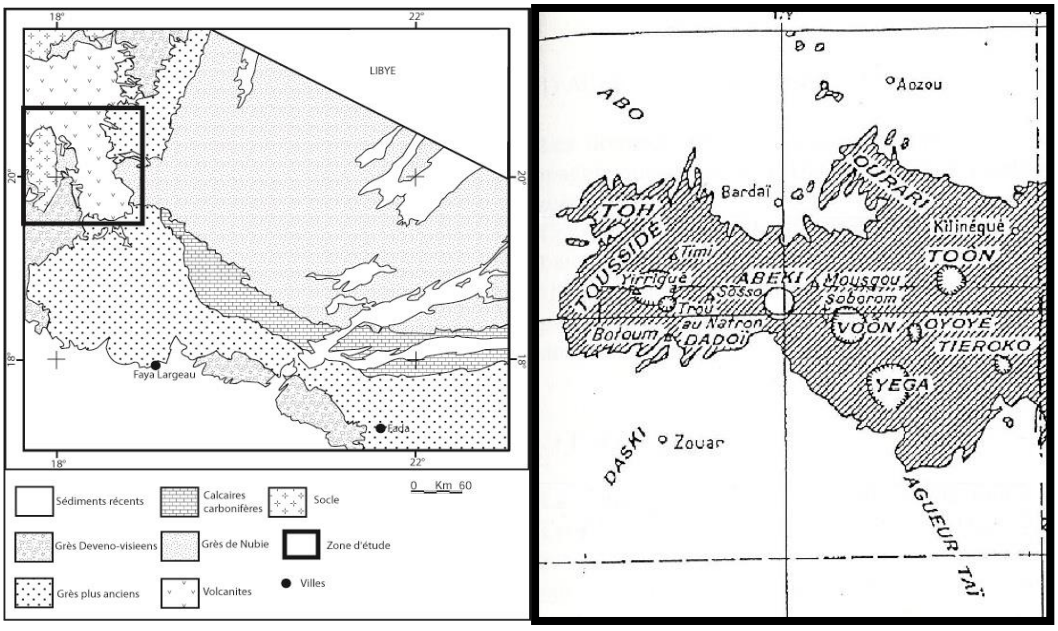

Figure 4. (A) Synthetic map of the geology of Tibesti (Doumnang, 2020); (B) Map of the Tibesti volcanic massif (Furon, 1963).

The lower series is composed of quartzites, gneisses, amphibolites and pyroxenites, and the upper series begins with a conglomerate, followed by shales, arkosic sandstones, rhyolitic metavolcanites and rare basalts (magmatic veins or sills) (Kaiser, 1972). Both series are traversed by granites with chemical affinities ranging from granodiorites and monzonites (related to pyroxenites) to calc-alkaline and alkaline composition, as well as by quartz and pegmatitic veins, with greenstone being the dominant rock (Dalloni 1934; Wacrenier et al., 1958; Pegram et al., 1976). Recent volcanic rocks are also present, with ages ranging from Lower Cenozoic to Lower Quaternary. The lithology is composed of a thick alkaline succession, including rhyolite, trachyte, phonolite, volcanic tuffs, ignimbrite and basalts, covering around 30,000 km2 (Vincent, 1963; 1995; Kaiser, 1972). At the western end of this volcanic complex is the Tarso Toussidé, a complex volcanic massif on the edge of the Pleistocene ignimbritic Yirrigue caldera. The highest point is the summit of the Toussidé stratovolcano, which is still active and produces numerous fumaroles and very young lava flows. The Tibesti formations have been dated using Rb-Sr and K-Ar radiometry, with ages ranging from 450 to 750 Ma (Vachette, 1964; Aschad et al., 1972; Schurmann, 1974; Pegram et al., 1976).
The little-explored Tibesti Precambrian basement has significant potential for metal mineralisation (fig. 5 B), mainly peri-plutonic mineralisations such as tin (Sn), tungsten (W), niobium (Nb), tantalum (Ta), beryllium (Be) and fluorine (F), in the Neoproterozoic plutonic domains, and base metal and/or gold mineralisations in the volcanic and sedimentary belts attributed to the Palaeoproterozoic (Hudeley et al., 1957; Chaussier, 1970; Kusnir 1993, 1995; Djekoundam, 1995; Kusnir and Kasser, 1997; Angel et al., 2010; 2011) (fig. 5 A).

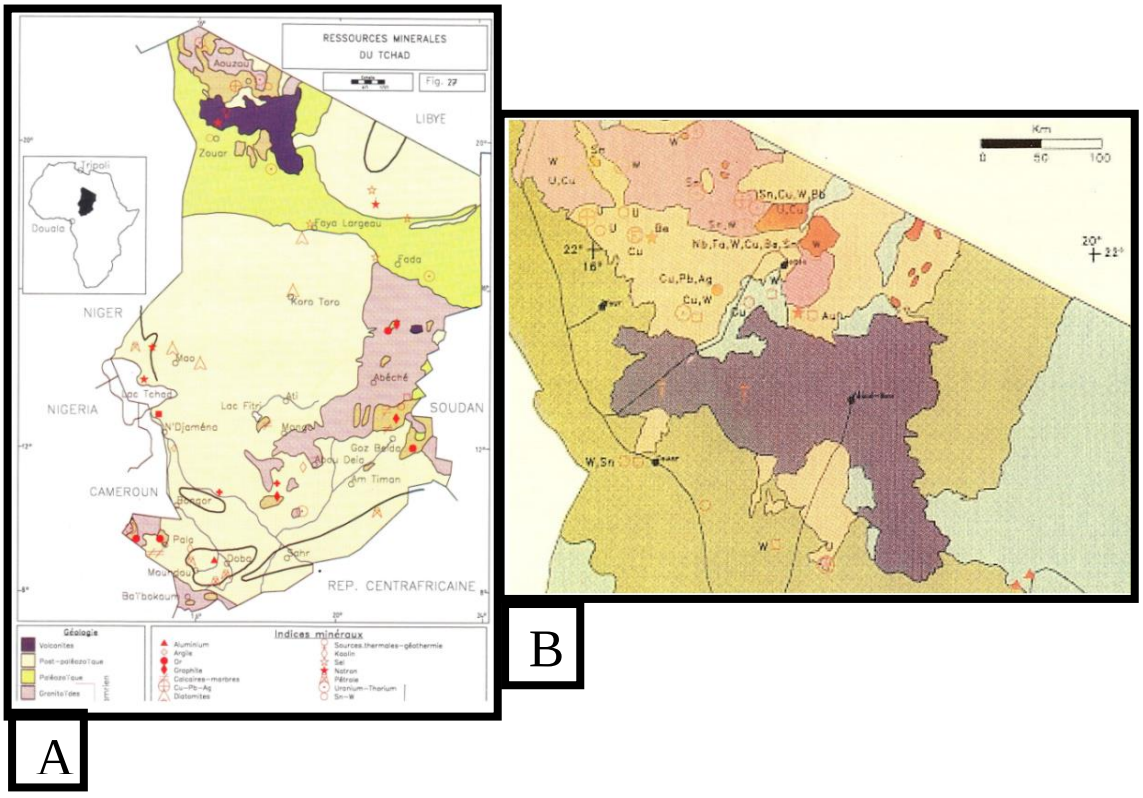

Figure 5. Map of mineral resources in Chad (A) and Tibesti (B). (Kusnir, 1995) ;

They are related to post-tectonic alkaline granites, appearing as stockworks of greisen or mineralised quartz veins and also pegmatite veins. They are mainly of the greisen type, with accumulations of cassiterite capped by quartz veins and stockworks, and sometimes gigantic crystals of wolframite (Chaussier, 1970; Kusnir, 1993; 1995; World Bank Group, 2023). In the 1930s, it was reported that 22 tetrametres of wolframite were collected directly from the surface of the Tibesti massif, without the need for digging. Their dimensions are sometimes impressive: at Yédri, seven pegmatite veins 4 km long were found with columbo-tantalite grades (47.5% Ta and 19.5% Nb) (World Bank Group, 2023) (fig. 5). The only known silver showing in Chad is at Ofouni, north-west of Bardai. It is associated with lead in polymetallic vein mineralisation. The presence of uranium (U) has also been detected in granites (Fig. 6), as well as in gold-bearing alluvium associated with metavulcanites (greenstone belts in the southern part of the Massif), and in hydrothermal veins for lead (Pb), zinc (Zn), copper (Cu), silver (Ag) and fluorine (F) (Hudeley et al,

Chaussier, 1970; Kusnir 1993; 1995; Kusnir and Moutaye, 1997; World Bank Group, 2023). Sedimentary uranium mineralisation is known at Bouboa, Ouadi Bakou near Fada. It is urano-thorianite in Cambro-Ordivician conglomerates, and in Ordivician sandstones at the base of the Tibesti. The potential for precious and semi-precious stones has also been mentioned (Kusnir 1993; 1995; Kusnir and Moutaye, 1997; World Bank Group, 2023).

Photos des orpailleurs sur les sites d'exploitation anarchique de l'or dans le Tibesti
Source: www.dw.com › fr ›

Photo 1. Photographs of gold panners at illegal gold mining sites in the Tibesti region.
Source : www.dw.com

III. MATERIALS AND METHODS

III.1. MATERIALS

To carry out this work, we used:
- Army aerial photography from 1930
- Landsat TM images, dated 07 March 1988
- Wollf geological map at 1:1500,000 scale
- Geological map and hydrogeological map by Schneider and Wolff, at 1:500,000.
- 1:200,000 topographic maps from the Institut Géologique National (IGN) of France.
- Exploration and mining maps of Borkou - Ennedi - Tibesti (BET) by Hudeley in 1957, B.E.T. n°30 of 20/11/57.
- Mineral resources map of Kusnir
- ENVI 4.5 software
- QGIS
- 3DEM software.

III.2. METHODS

Landsat TM images with 30 m resolution, Geotiff format, dated 07 March 1988;
Merging of the two images to obtain the best viewing angles;
Display of shading;
Landsat image processing in ENVI 4.5, colour composition, channel ratio.
Application of the Lapalacian/QGIS filter;
Creation and overlay of a 'vector layer' on the filtered image.
Vectorisation of the lineaments highlighted by the Lapalacian filter;
Processing of the 30 m resolution SRTM1 image in QGIS for altitude variation;

IV. REMOTE SENSING

Remote sensing is the set of techniques used to observe, analyse and interpret data acquired at a distance. The main objective of this work is to demonstrate that it is possible to make valid and systematic petrographic deductions from TM data covering desert areas. The techniques recommended are simple and are based on the identification of spectral reflectance characteristics common to many types of rock (Scanvic, 1983; 1992; Baghdadi et al., 2005).

IV.1. DATA ACQUISITION, PROCESSING AND ANALYSIS

IV.1.1. Data acquisition

The data used are those from the Landsat Thematic Mapper 5° version (Landsat TM) satellite launched in March 1984. Landsat 7 is one of the 2nd generation satellites with improved resolution of 30 m and 7 channels, with the possibility of acquisition in the mid-infrared range. A scene acquired by the Landsat TM satellite covers 185 km by 185 km, with seven broad spectral bands. Six of these bands detect visible and reflected infrared radiation (0.45 to 2.35 µm) and have a spatial resolution of 30 x 30 m (Scanvic, 1983, Sultan, et al., 1987). The data were acquired on 07 March 1988 and referenced 184/46. These data were downloaded to the SIGEO laboratory, Centre de recherche et d'enseignement
des géosciences de l'environnement at Aix Marseille University.

IV.1.2. processing

Image processing is carried out to enhance the image, make certain structures appear or disappear and enable easy recognition or analysis of the objects sought (Stock, 1972; Mohamed and Seyd, 1982; Scanvic, 1983; 1992; Mohammad, 1986; Bonneville, 1992; Baghdadi, 2005).

Stretching

This is an adaptation of the dynamics. It consists of spreading the limits of the histogram from 0 to 255. Using ENVI 4.5 software, this treatment makes it possible to brighten the raw image and analyse it easily. It was carried out on several coloured composites, but TM7-TM4-TM3 and TM7-TM4-TM2 give more information about the lithology of the rocks in the area and the circular to subcircular structures of the volcanoes (fig. 6).

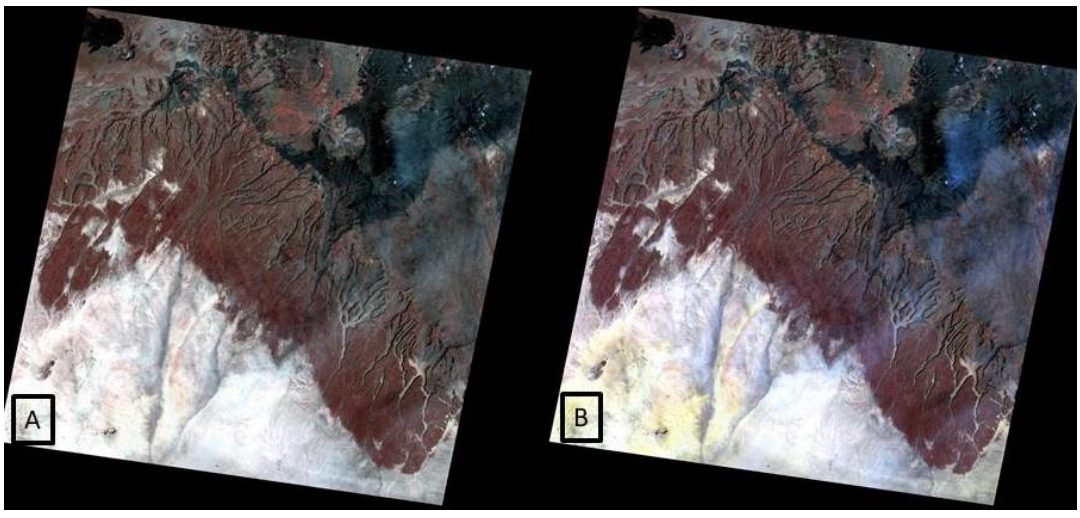

Figure 6: TM7, TM4, TM3 colour compositions (A); TM7, TM4, TM2 (B).

The ratio

This is a ratio of two or more channels. The ratio eliminates topographical effects and enhances the low reflectance of rocks in the shade (sultan et al., 1987). This increases the possibility of identifying different lithological formations. Two channel ratios were established: TM2/TM7 and TM4/TM7 (fig. 7).

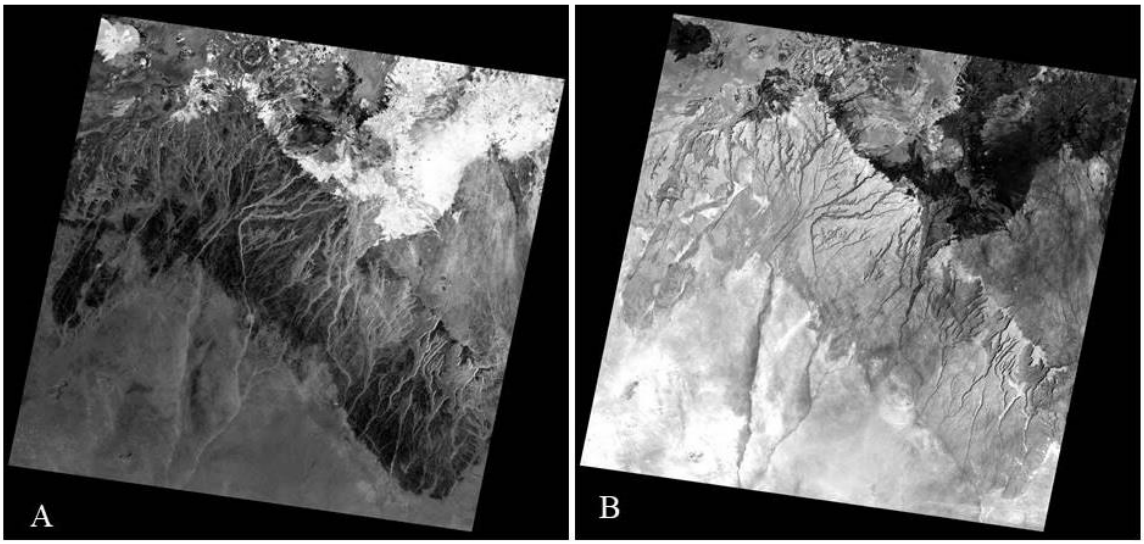

Figure 7: TM2/TM7 (A) and TM4/TM7 (B) channel ratios.

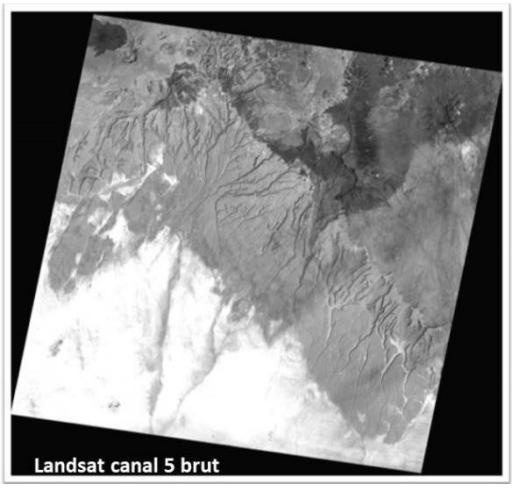

Figure 8. Landsat TM 5 raw, already showing sand deposits thanks to the very high reflectance of the sand.

This figure already shows a preliminary lithology of the geological formations at different reflectances.

Filtering

This is an image processing programme that eliminates noise, sieving or superficially scanning the image to reveal certain hidden or difficult-to-identify structures. For our work, we used the Laplacian filter via filtering with the 3*3 mask in QGIS 3.28 (fig. 9).

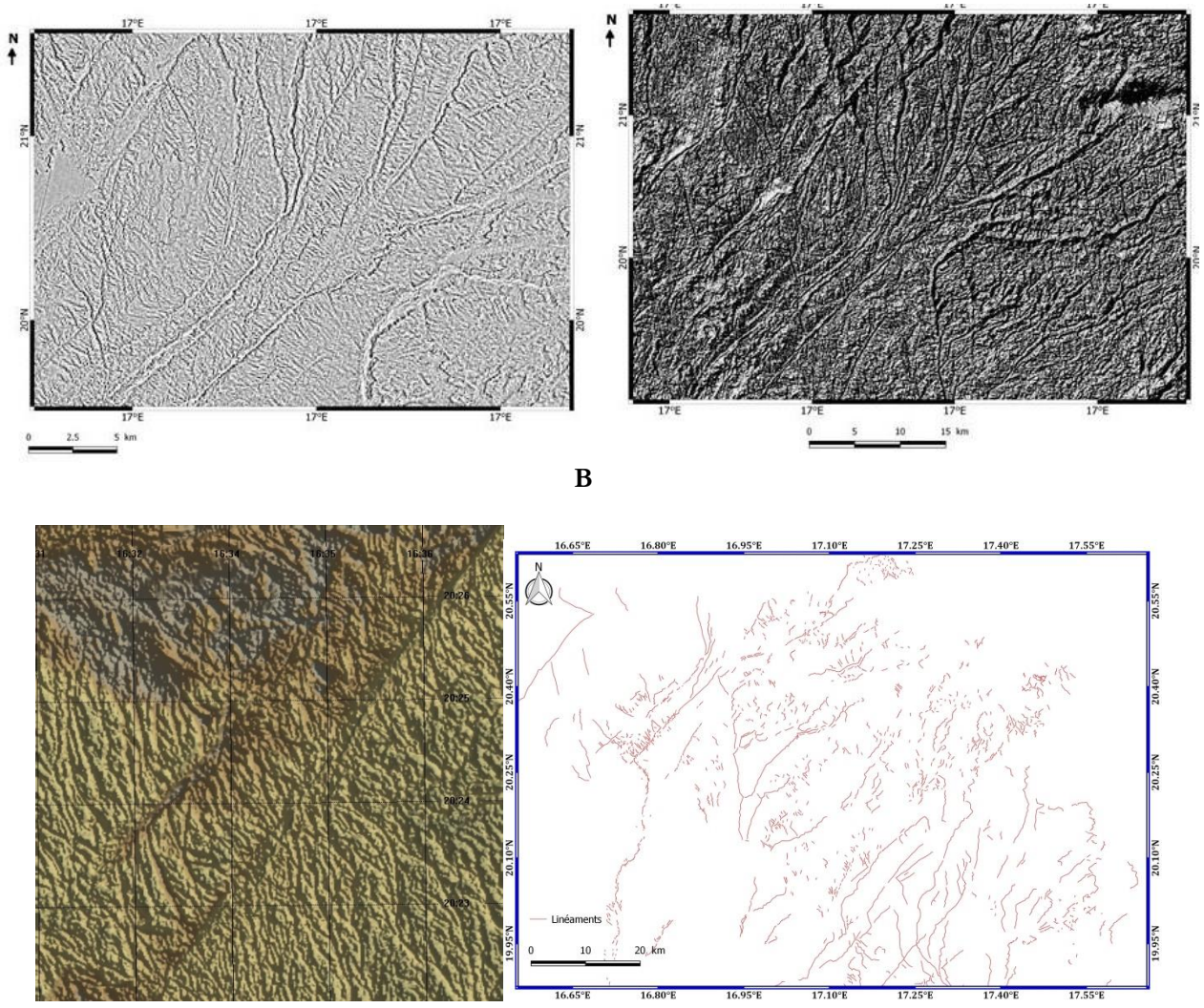

Figure 9 (A). Extract of the image using the Laplacian filter (B). Shading applied to the same area. (C). 3 DEM applied to the Lansat image (C). Linear map of the study area after filtering with the 3*3 mask, using QGIS 3.28.

IV.1.3. Analysis

This is the description of the lithological layers recognised in the various channels processed and the interpretation of the tectonic structures (faults, fractures, lineaments, folds, etc.).

The document is organised as follows: firstly, the lithological verification of spectral reflectance data for the dominant rock types exposed in the massif and defining them. TM data and complementary aerial photographs are then discussed, with emphasis on processing and preservation procedures that emphasise the dominant petrographic controls for Tibesti rocks, while minimising spectral variations due to topography. The results of the various Landsat TM data processing operations and the compilation of old maps have enabled us to update the geological map of the study area. Lineament extractions were used to identify faults and folds and to draw up a structural diagram.

The Precambrian

Two metamorphic formations (Upper Tibestian and Lower Tibestian) and granites make up the Precambrian.

- Upper Tibestian: this outcrops in large patches to the south of the Tarso Tiékoro, to the east of the Tarso Yéga and in the valleys draining the south of the massif. The Upper Tibestian consists of shales, sandstones and conglomerates (Doumnang, 1995). The V-shaped structure in relation to the watercourses shows that the shales dip eastwards. The Precambrian schistosity is oriented north-south. Numerous folds have been observed (fig.6 A and B). These are tight folds, parallel to the plane of the schistosity, isoclinal and probably synschistose, as the planes of the schistosity intersect the hinge of the folds. The radii of curvature of these planes vary. A coloured composition of channels 7, 4, 2, shows the Upper Tibestian in yellowish-brown with a fine striated texture. The shales are made up of dark and light banks (fig. 6 A and B). This ensemble appears to outcrop to the west of Tarso Voon, around the Tarso Abeki crater.

Two types of drainage system can be identified from the sediments they drain. The first type flows from north-west to south-east and contains volcanic sediments; the second type has a varied flow direction and is characterised by alluvium derived from sandstone.

The Lower Tibestian: this takes the form of a lens running north-west-south-east, to the south of the Tarso Tiékoro (Fig. 7 A). The schistosity is not oriented in the same way as that of the Upper Tibestian, but follows the direction of the entire formation.

The boundary between the Upper and Lower Tibestian is marked by a white band (Fig. 7 A). This white band is characteristic of a fault corridor. This fault corridor seems to represent a crushing zone showing the presence of mylonites.

Granites: these are circular in shape. They are intrusive granites. These intrusions are greater than 1 km in diameter (fig. 7 A and B). Around these circumscribed granites, the schistosity disappears and a halo of metamorphism develops, which seems to correspond to hornfels. This halo, for each granite, has an irregular outline and is between 100 and 150 m wide. These are syntectonic granites (Doumnang, 1995).

The Paleozoic

This covers most of the southern part of the massif. These are soft sandstones with oblique stratification. Erosion at the weakest points of this rocky mass has favoured the establishment of the hydrographic network. The erosion-resistant sandstone formations give the Palaeozoic a dark (Fig. 6 A) or light grey (Fig. 6 B) tabular and irregular structure, oriented NW-SE. These subhorizontally dipping formations are interspersed with fractures running in all directions. The Palaeozoic is unconformably underlain by Precambrian formations (Figs. 5, 6).
The hydrographic network distinguishes two types of sandstone formation.

The first type is made up of soft sandstone. The hydrographic network is extensive and creates canyons.

The second type, which outcrops in the southern part of the area, is covered by a thin layer of sand and may be made up of clayey sandstone. The hydrographic network has a dendritic structure.

Tertiary-Quaternary

This corresponds to volcanic formations (Vincent, 1963).

Rhyolites: these form the bedrock of the volcanic formations. They are found around Pic Toussidé and Tarso Voon. The rhyolites observed in Tarso Yéga have the appearance of a viscous flow characteristic of silica-rich lavas. These formations have a very high reflectance and a characteristic whitish hue (Fig. 6 A). The rhyolitic formations are underlain by Palaeozoic rocks.

Basaltic lavas: these are found in the vicinity of volcanoes and are therefore not as widely distributed as rhyolites. They also outcrop in valleys.

Trachy-andesites: these rocks are widespread in and around the Pic Toussidé crater (Fig. 6 A and B; 7 A and B). They contain an apparently fresh lava flow. They are very homogeneous and have no particular texture.

Sands and dunes: these cover the Palaeozoic sandstones in the southern part of the study area, and mark the northern limit of the Chadian basin. Thanks to their very pronounced reflectance due to the high silica content, they are conspicuous in Figures 6, 7 and 8. They are probably aeolian sands that have progressed northwards over the last 20 years.

Alluvial deposits: these are found in volcanic craters and watercourses; their reflectance varies according to their origin: low for alluvial deposits of volcanic origin and high for alluvial deposits of sandstone origin (Maley et al., 1970).

The results of these analyses and interpretations have enabled us to produce a geological map of the southern Tibesti massif.

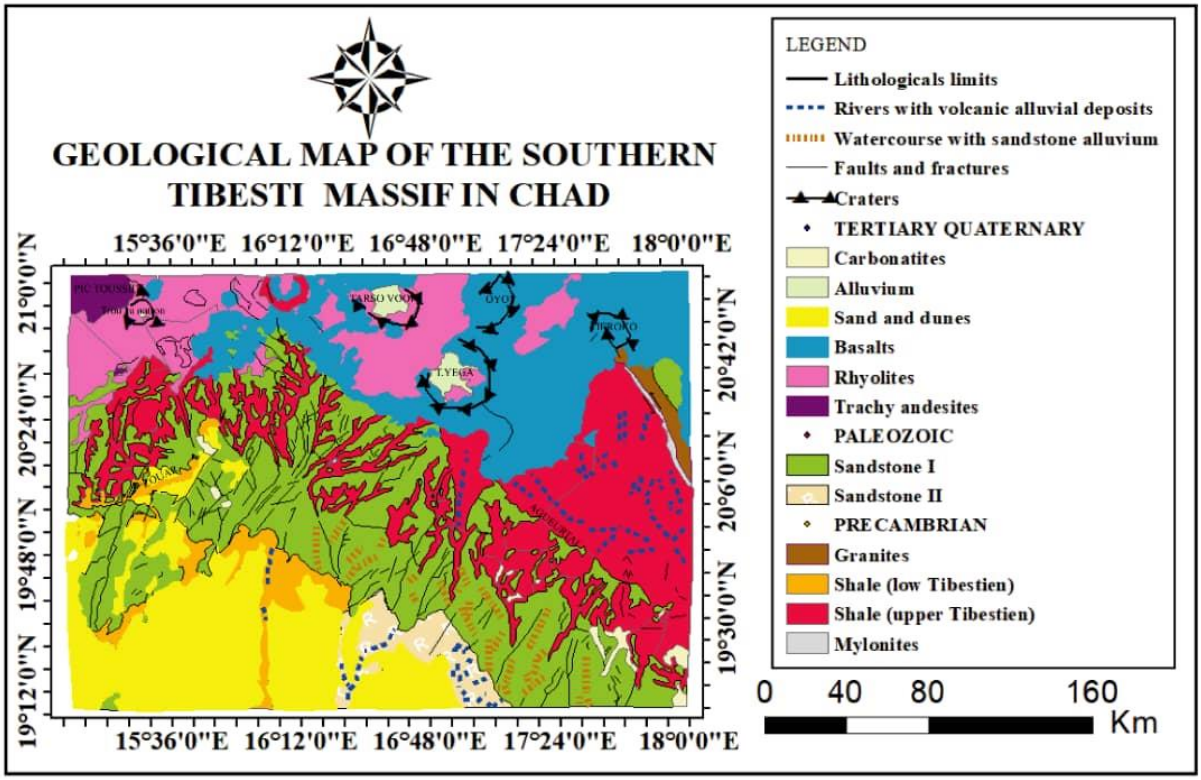

Figure 10: Geological map of the southern Tibesti massif

Tectonics

The various image processing operations have identified several fault families.

- NE-SW faults are the most abundant and remarkable (Guiraud et al., 1985). They can be seen to the west of the image. These are multiphase normal faults; deposits of eolian sands can be seen on the subsided compartments.

- North-South trending faults.

- NW-SE faults are fewer in number but still important. The most important is the one that marks the Upper Tibestian-Lower Tibestian boundary. This major fault probably played a role from the end of the Precambrian to the Tertiary, as it cuts through the Precambrian shales and disappears beneath the recent Tarso Tiékoro formations (figs. 6 and 7 A).

Analysis of the folds, planes of schistosity and lineaments on either side of the fault suggests that this fault acted as a senestial shear at the end of the Precambrian. This senestial shear has a long and complex history. It was

responsible for the uplift of the Lower Tibestian and the apparent senestial offset of the formations. It appears to be a continuation of the great Aswa fault (Gaulon et al., 1990; 1991; Guiraud et al., 2000).

The straight NW-SE ridge of the Aguertaï cliff limits the Precambrian formations to the north and the Palaeozoic tabular platform to the south. This cliff is extended to the north-west by a succession of faults in the same direction.

The NE-SW, North-South trending faults are, in general, normal faults with slight rejection and polyphase play (Fig. 6 C) (Guiraud et al., 1985; 1987; 1992).

The faults appear to play a role in the location of volcanism in Tibesti. The Tibesti massif is linked to Quaternary volcanism (Vincent, 1963).

The faults that affect this massif belong to individualised families at the scale of Central Africa. The NW-SE and NE-SW faults are thought to be the N140 and N20 faults described previously (Guiraud et al., 1985; 1987; 1992; Gaulon et al., 1990; 1991; Guiraud et al., 2000; Guiraud et Maurin, 1991). According to these authors, these faults came into play several times and in different ways during the Lower Cretaceous. The lineament map and the structural data analysed and interpreted make up a structural diagram (fig. 11).

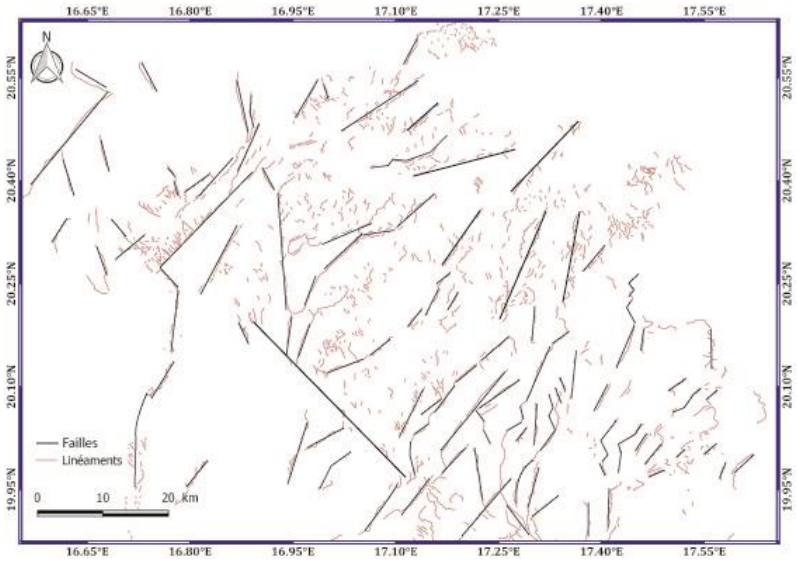

Figure 11: Structural diagram of the southern Tibesti massif

CONCLUSION

Geological surveys using remote sensing are now operational. It can be used in most regions, whether in forested areas or desert zones, as in the case of Tibesti, where access is difficult because of the hostility of nature on the one hand and political events on the other.

Satellite images are an additional analytical tool for the geologist in that they provide sufficient information on the geomorphology and structural geology of the study area.
All this information obtained from the various processes, analyses and interpretations has led to the production of an updated geological map of southern Tibesti and a structural diagram.

It is now possible to obtain maps, with good reliability and low uncertainties, covering vast areas, maps obtained in a very short time, with less field work, in economically interesting and difficult-to-access areas.

Acknowledgements

We would like to express our sincere thanks to the French Embassy in Chad, which funded a high-level scientific visit (SSHN). Our thanks also go to the colleagues who agreed to invite us to their laboratory at the Centre de Recherche et d'Enseignement des Géosciences de l'Environnement (CEREGE), Aix-Marseille University in Aix-en-Provence (France), despite their heavy workloads, not forgetting the various team leaders and staff at CEREGE.

REFERENCES

1. Abdelsalam, G., M., Liégeois, Paul, J., Stern, J., R., 2002. The Saharan Metacraton. J. African Earth Sci. 34, 119–136. https://doi.org/10.1016/S0899-5362(02)00013-1
2. Abdelsalam, M.G., Gao, S.S., Liégeois, J.P., 2011. Upper mantle structure of the Saharan Metacraton. J. African Earth Sci. 60, 328–336. https://doi.org/10.1016/J.JAFREARSCI.2011.03.009
3. Angel J.M., Arregros M., Augé T., Billa M., Genna A., Gouin J., Lebret P., Marteau P., Pouget A.M.,Tourlière B., (2010). Développement et promotion du secteur minier de la République du Tchad, Rapport BRGM/RC-58519-FR, 96 pp.
4. Angel J.M., Arregros M., Augé T., Billa M., Genna A., Gouin J., Lebret P., Marteau P., Pouget A.M.,Tourlière B., (2011). Carte geologique et des ressources minerales de la République du Tchad. Conference: 23rd Colloquium of African Geology At: Johannesburg Volume: Abstracts Volume; "Together in Africa for a leading role in geoscience"https://www.researchgate.net/publication/258240766_carte_geologique_et_des_ressources_minerales_de_la_republique_du_tchad#fulltextfilecontent [accessed Jun 24 2024].
5. Baghdadi,N., Grandjean, G., Lahondère, D., Paillou, P., Lasne, Y., (2005). apport de l'imagerie satellitaire radar pour l'exploration géologique en zones arides. C. R. Geoscience 337 (2005) 719–728.
6. Bertrand, JML, Caby, R. (1978) Évolution géodynamique de la ceinture orogénique panafricaine : une nouvelle interprétation du bouclier du Hoggar (Sahara algérien). *Geol Rundsch* **67** , 357–388 (1978). https://doi.org/10.1007/BF01802795.
7. Bessoles, B. & Trompette, R., (1980). La chaîne panafricaine. Zone mobile d'Afrique centrale (partie sud) et zone soudanaise. Mémoire du Bureau de Recherches Géologiques et Minières, Orléans.
8. Bonneville, A. (1992). La surveillance des volcans par satellite. La Recherche, 242. Vol. 23, pp. 404-413.
9. Bruschek, G. J. (1974). Zur geologie des Tibesti (zentral Sahara). Forschungsstation Bardaï FU-Geoloen in der zentralsahara. Pressedienst wissenschaft, 5. Freien Universität Berlin,pp. 15-35.
10. Bruschek, G. J. (1982). Zur geologie des zentraltibesti. Berliner Geogr. Abhandlungen, 32, pp. 85-98. Berlin.
11. Chaussier, J.B. (1970). Carte minérale du Tchad & notice. Rapport inédit 68p. Direction des Mines et de la Géologie, Fort Lamy (N'Djaména)
12. Dalloni M., (1932). Une mission scientifique au Tibesti (1930-1931) [Texte imprimé] / Publication : [S.l.], [1931-1932] Note(s) : Extr. des : "C.R.Ac.Sc.", Paris, 26 Octobre 23 Novembre 1931, 1er février, 15 février 1932, 16 p.
13. Dieter, J. (1982). Bemerkungen zur geologischen alterseinstufung des Tibesti-vulkanismus und des Bardaï-sandsteins nach kalium-argon-datierungen. Berliner Geographische. Abhandlungen, 32, Berlin. pp. 133-142.
14. Djekoundam, M. (1995). Géologie et Potentiel Minier du Tchad. Ministère des Mines, de l'Energie et du Pétrole. N'Djaména Tchad, 1995.
15. Djerossem, F., Berger, J., Vanderhaeghe, O., Isseini, M., Ganne, J., Zeh, A., (2020). Neoproterozoic magmatic evolution of the southern Ouaddaï Massif (Chad). Bull. la Société Géologique Fr. 191, 34. https://doi.org/10.1051/BSGF/2020032
16. Doumnang, J-C. 1995. Cartographie géologique du Sud massif volcanique du Tibesti (Tchad) à partir d'image satellite Landsat TM. Mémoire de D.E.S.S Université Paris VI. 24 p.
17. Engel J. L. et Weinstein O., (1982). The Thematic Mapper – Overview in International Geoscience and Remote Sensing Symposium, Munich, 1982. Digest : Institute of Electrical and Electronics Engineers. V. I. P. WPI. 1 – 1.7.

18. Gérard, J. (1963). Notice explicative sur la feuille Bossangoa - est. Carte géologique de reconnaissance à l'échelle du 1/500,000. Levés effectués de 1950 à 1957. IGN, République centrafricaine.
19. Guiraud, R. Bahay, I. et Bellion, Y. (1985). Les linéaments guinéo-nubiens: un trait structural majeur à l'échelle de la plaque Africaine; note présentée par Aubouin, J. Académie des Sciences de Paris, 300, Série II, N° 1, pp. 17-20.
20. Guiraud, R. Bellion, Y. Benkhenlil, J. and Moreau, C. (1987). Post-hercinian tectonics in Northern and Western Africa. Geological journal, 22. Thematic issue, pp.433-466.
21. Guiraud, R. et Maurin, J-C. (1991). Le rifting en Afrique au Crétacé inférieur: synthèse structurale, mise en évidence de deux étapes dans la genèse des bassins, relations avec les ouvertures océaniques péri-africaines. Bulletin Société Géologique de France, 162, N° 5, pp. 811-823.
22. Guiraud, R. Binks, R.M. Fairhead, J.D. and Wilson M. (1992). Chronology and geodynamic setting of Cretaceous-Cenezoic rifting in West and Central Africa. In P.A. Ziegler (editor), Geodynamics of rifting, volume II. Case History studies on Rifts: North and South America and Africa. Tectonophysics, 213: pp.227-234.
23. Guiraud, R. et Maurin, J-C. (1992). Early Cretaceous rifts of Wesyern and Central Africa: an overview. In P.A. Ziegler (editor), Geodynamics of rifting, volume II. Tectonophysics, 213: pp. 153-168.
24. Gupta, R.P. (1991). Remote sensing geology. Springer verlag. pp. 223-309 Berlin.
25. Hisseine Mahamoud A., (1986). Geologie und hydrogeologie des Erdis - Beckens NE - Tschad. Berliner geowissenschalftliche abhandlungen. A 76, 67 p. Berlin.
26. Hudeley H., Vincent P., Wacrenier Ph., (1957). Rapport de fin de mission 1956-1957 : mission d'exploration géologique et minière des confins nord du Tchad (Borkou-Ennedi-Tibesti). Direction des Mines et de la Géologie. [Brazzaville]. Format : 2 vol. (166 p.) ; 27 cm + 2 cartes en coul.
27. Hunt, G.R. Salisbury, J.W. and Lenhoff, C.J. (1973). Visible and near infrared spectra of minerals and rocks: vol. II. Acidic igneous rocks. Modern Geology, 4, p. 217-224.
28. Hunt, G.R. Salisbury, J.W. and Lenhoff, C.J. (1974). Visible and near infrared spectra of minerals and rocks: IX. Basic and ultrabasic igneous rocks. Modern Geology, 5, p. 15-22.
29. Gaulon, R. Chorowicz, J. Vidal, G. Romanowicz, B. Roult, G. (1990). Regional geodynamic implications of May-July 1990 earthquake sequence in southern Sudan. Tectonophysics, 209, pp. 87-103.
30. Gaulon, R. Chorowicz, J. Romanowicz, B. (1991). Les séismes du Sud-Soudan de mai-juillet 1990: évidence d'une transformante continentale active. Compte rendu de l'Académie des Sciences de Paris, 312, Série II pp. 377-384.
31. Isseni M, (2011). Croissance et différenciation crustales au Néoprotérozoïque. Exemple du domaine panafricain du Mayo Kebby au Sud-ouest du Tchad. Thèse doct. Université Henri Poincaré.345p.
32. Kaiser, K. (1972). Der Kanozoische vulkanismus im Tibesti-Gebirge. Berliner Geogr. Abhandlungen, 16, Berlin. pp. 9-34.
33. Kasser M.Y. (1998). Le Précambrien tchadien: l'exemple du Mayo- Kebbi, in Mbaguedje, D. (2015). Métallogénie de l'or et de l'uranium dans le cadre de la croissance et de la différenciation de la croûte au Néoprotérozoïque: Exemple du massif du Mayo-Kebbi (Tchad) dans la Ceinture Orogénique d' Afrique Centrale. Thèse de Doctorat, Université de Lorraine (France), 269 pp.
34. Kusnir, I., (1993). Ge□ ologie, ressources mine□ rales et ressources en eau du Tchad. Revue du Centre national d'appui à la Recherchee, en français – 1ère éd. 100pp.
35. Kusnir, I., (1995). Ge□ ologie, ressources mine□ rales et ressources en eau du Tchad. Revue du Centre national d'appui à la Recherche, en français – 2ème éd. Actualisée et augm. 115pp.
36. Kusnir, I., Moutaye H.A., (1997). Ressources minérales du Tchad: une revue, J. Afr. Earth Sci. 24 (1997) 549–562.
37. Louis, P., (1970) - Contribution géophysique à la connaissance géologique du bassin du lac Tchad Mem. ORSTOM, 42, 311 p. t annexe
38. Maley, J., Cohen J., Faure H., Rognon P., Vincent P. M., (1970). Quelques formations lacustres et fluviatiles associées à différentes phases de volcansismes du Tibesti (Nord du Tchad). Cah. ORSTOM, Ser. Géol. (1970), II, I, 127 – 152.
39. Mbaguedje D, (2015). Métallogénie de l'or et de l'uranium dans le cadre de la croissance et de la différenciation de la croûte au Néoprotérozoïque : Exemple du massif du Mayo-Kebbi (Tchad) dans la Ceinture Orogénique d'Afrique Centrale. Uniersité de Lorraine, Nancy, Thèse doct.270p.

40. Mohammad, H. S. (1986). Lithologiche und tektonische Auswretung von Landsat-MSS-Daten und Luftbildern aus dem Tibesti-Gebirge / Zentralsahara mit hilf visueller und digitaler klassifizierungsverfahren. Berliner Geowissenschaftliche Abhandlungen, A 69, Berlin. 80p.
41. Mohammad, H. S. Seyd, R. H. M. T. (1982). Eine photogeologische Luftbildauswertung nordlich und sudlich des Enneri Dilenao im Tibesti-Gebirge / Zentralsahara, Tschad. Berliner Geogr. Abhandlungen, 32, Berlin. pp. 98-132.
42. Pegram, W. J., Register, J. K., Fullagar, P. D., Ghuma, M. A., Rogers, J. J. A., (1976). Pan-african ages from a Tibesti massif batholith, Southetern Libya. Earth and Planetary Science Letters. 30 (1976), 123 – 128.
43. Maurin, J-C. and Guiraud, R. (1993). Basement control in development of the Early Cretaceous West and Central African Rift System. In P.A. Ziegler (editor), Geodynamics of rifting, volume II. Tectonophysics, 228: pp. 81-95.
44. Scanvic, J-Y.(1983). Utilisation de la télédétection dans les Sciences de la Terre. Manuels et méthodes 7. Bureau de Recherches Géologiques et Minières, Orléans, 158 p.
45. Scanvic, J-Y.(1992). Télédétection Aérospatiale et informations géologiques. Manuels et méthodes 23. Bureau de Recherches Géologiques et Minières, Orléans, p.
46. Schneider, J.L. et Wolff, J.P. (1992). Carte géologique et cartes Hydrogéologiques à 1/1.500.000 de la République du Tchad: mémoire explicatif. Bureau de Recherches Géologiques et Minières, 209. 1 et 2. 921 p.
47. Schurmann H. M. E. (1974). The Precambrian in North Africa (E. J. Brille Leiden 1974) 79
48. Aschad A. H., Sayya T. A., El Kholy S. B., Youssef A. (1972). Rb – Sr isotopic age determination of some basament Egyptian granites. Egypt J. Geol. 16 (1972) 269.
49. Stock, P; (1972). Photogeologische und tektonische Untersucungen am Nordrand des Tibesti-Gebirges, Zentral-Sahara, Tschad. Berliner Geogr. Abhandlungen, 14, Berlin. 55 p.
50. Sultan, M., Ardvison R. E., Sturchio, C. N. Guiness, E. A., (1987). Lithologic in arid regions with Landsat thematic mapper data : Meatiq dome, Egypt. Geological Society of America Bulletin, V 99. P. 748 – 762. 14 figs, 3 tables, December 1987.
51. Vachette, M. (1964). Age radiométrique des formations cristallines d'Afrique Equatoriale. Ann. Fac. Sci. Clermont – Ferrand 25 Ser. Geol. 8. Etudes Géochronol, 1 (1964) 31.
52. Vincent, P.M. (1963). Les volcans Tertiaires et Quaternaires du Tibesti occidental et central (Sahara du Tchad). Bureau de Recherches Géologiques et Minières, 23. Paris, 307 p.
53. Wolff, J.P., 1964. Carte Géologique de la République du Tchad. Echelle 1/1.500.000. Bureau de Recherches Géologiques et Minières, Paris.
54. **World Bank Group. Rapport diagnostique du secteur minier du Tchad. (2023).** www.worldbank.org